Star-Like Polypeptides as Simplified Analogues of Horseradish Peroxidase (HRP) Metalloenzymes

Antoine Tronnet, Pedro Salas-Ambrosio, Rosa Roman, Lourdes Monica Bravo-Anaya, Marcela Ayala, Colin Bonduelle

RESEARCH ARTICLE

Macromolecular Bioscience
www.mbs-journal.de

Star-Like Polypeptides as Simplified Analogues of Horseradish Peroxidase (HRP) Metalloenzymes

Antoine Tronnet, Pedro Salas-Ambrosio, Rosa Roman, Lourdes Monica Bravo-Anaya, Marcela Ayala, and Colin Bonduelle**

Peroxidases, like horseradish peroxidase (HRP), are heme metalloenzymes that are powerful biocatalysts for various oxidation reactions. By using simple grafting-from approach, ring-opening polymerization (ROP), and manganese porphyrins, star-shaped polypeptides analogues of HRP capable of catalyzing oxidation reactions with H_2O_2 is successfully prepared. Like their protein model, these simplified analogues show interesting Michaelis–Menten constant (K_M) in the mM range for the oxidant. Interestingly, the polymer structures are more resistant to denaturation (heat, proteolysis and oxidant concentration) than HRP, opening up interesting prospects for their use in catalysis or in biosensing devices.

1. Introduction

In living systems, metalloenzymes play critical roles in biological processes by harnessing the unique chemical properties of metal ions to catalyze and regulate biochemical reactions.[1] Heme proteins[2] are those composed of a protein matrix and a heme cofactor that plays a predominant role in numerous biological mechanisms, such as O_2 binding and transport,[3] electron transfer[4] and oxidation of certain substrates.[5] Generally, heme proteins can catalyze oxidation reactions, and they can be divided into two main protein families depending on the oxidizing agent involved: oxygenases, which use O_2, and peroxidases, which use H_2O_2 or other peroxide compounds.

Peroxidases are enzymes found in a wide range of living organisms, but also are powerful catalytic tools for chemists.[6] Peroxidases contain a heme group that acts as a transient electron donor during the oxidation reactions, which typically involves the transfer of electrons from the substrate to the peroxide, resulting in the formation of water and an oxidized product. The most widely studied peroxidase in catalysis is horseradish peroxidase (HRP). This enzyme is commonly used in diagnostic assays, molecular biology techniques, and as a marker in immunohistochemistry.[7] It can be used for polymerization,[8] coupling,[9] hydroxylation,[10] or nitration reactions.[11] However, the use of these enzymes is limited by significant constraints including a lack of stability over time. It has to be stored under specific temperature conditions (ideally at 4 °C for instance) to preserve the protein structure, and the enzyme is only active under physiological conditions (specific pH and ionic concentration). What is more, despite its extraordinary catalytic capacity, the enzyme is difficult to recycle, and its use is often one-off. To overcome this problem, many research has been carried out to develop synthetic analogues of metalloenzymes possessing peroxidase-like activity.[12] Indeed, replacing HRP by chemical catalysts may present some key advantages such as imparting thermal stability, decreasing substrate selectivity, improving catalytic activity, etc. These artificial systems should be designed to have similar structural and functional features to natural peroxidases, allowing them to catalyze oxidation reactions. This includes the development of artificial nanomaterials with peroxidase-like activities,[13] reconstituting the porphyrin core of peroxidases with porphyrins that can coordinate different metals, such as manganese porphyrins.[14] To better recreate the active site surroundings the prosthetic group, the use of small but sequence-controlled peptides is a particularly relevant approach with oxidation catalytic activities similar to those of natural enzymes.[15] Numerous approaches have been already developed in this direction, including incorporating non-natural

A. Tronnet, P. Salas-Ambrosio, C. Bonduelle
CNRS
LCPO (Laboratoire de Chimie des Polymères Organiques (UMR5629))
University of Bordeaux
Bordeaux INP, 16 avenue Pey Berland, Pessac F-33600, France
E-mail: colin.bonduelle@u-bordeaux.fr

A. Tronnet
CNRS
LCC (Laboratoire de Chimie de Coordination (UPR8241))
University of Toulouse
205 route de Narbonne, Toulouse F-31077, France

R. Roman, M. Ayala
Departamento de Ingeniería Celular y Biocatálisis
Instituto de Biotecnología UNAM. Av. Universidad 2001
Col. Chamilpa, Cuernavaca, Morelos
E-mail: marcela.ayala@ibt.unam.mx

L. M. Bravo-Anaya
University of Rennes
Institut des Sciences Chimiques de Rennes
CNRS
Rennes UMR6226, France

The ORCID identification number(s) for the author(s) of this article can be found under https://doi.org/10.1002/mabi.202400155

DOI: 10.1002/mabi.202400155

amino acids and non-native cofactors into native or *de novo* protein scaffolds.[16]

In this stimulating context, peptide polymers are macromolecules that consist of one or more amino acid(s) that are randomly repeated several times. These synthetic polypeptides are obtained by ROP of *N*-carboxyanhydrides (NCA): the advantage of this method is that polypeptides presenting the size of a protein can be obtained in a single step. Also, those polypeptides combine advantageous features of synthetic polymers (solubility, processability, rubber elasticity, etc.) with those of natural proteins (secondary structure, functionality, biocompatibility, etc.).[13] A very interesting point is that the ROP of NCAs paves the way to various topologies (cyclic, branched, conjugates, etc.) that would be difficult to implement using other preparation methods (biotechnology, solid-phase synthesis, etc.).[17] For instance, the ROP of NCA gives access to star polymers, i.e., macromolecules with elongated polymeric arms that have very low entanglement as compared to cyclic and linear polymers.[18] On another hand, polypeptides are ideal macromolecules for mimicking the structural properties of natural proteins. For example, these polymers can create local secondary structures via the interplay of hydrogen bonds in the form of α-helices or β-sheets.[19] Moreover, combining polypeptide polymers with coordination chemistry has already permitted to mimic the metal-induced secondary structures of metalloproteins with some selectivity[20]: for example when it involves poly(*L*-glutamic acid), metal-induced structuring could only be done with Zn^{2+} or Cd^{2+}.[21] On the surface of metallic nanoparticles, this coordination-induced structuring enables the preparation of nanocomposites with advanced properties, in which polymers reproduce the dielectric properties of natural proteins.[22]

In this work, we present a new possible relevance of combining polypeptides polymers with coordination chemistry to mimic the catalytic activity of HRP. Inspired by the protein model, star-shaped metallopolypeptides with different polymer lengths have been prepared in two steps by grafting from a manganese porphyrin core. The obtained polymers were fully characterized by a combination of NMR, SEC and spectroscopic analyses, in order to determine the structure, molar mass and dispersities. They were then studied as polymeric analogues of HRP in oxidation reactions to better understand the influence of the polypeptide part surrounding the heme on the catalytic efficacy. Beside the water solubility introduced by the polypeptide blocks, the star-shaped topology also showed that the catalytic activity was significantly influenced by the polymeric length (k_{cat}, K_M) with much greater resistance than the natural enzyme to changes in temperature or H_2O_2 concentration.

2. Results and Discussion

2.1. Synthesis and Characterization of Mn-Porphyrin Grafted Polypeptides

An intriguing aspect of the ROP of NCA monomers is that it enables easy access to star-shaped polypeptides. These polypeptides are elongated amino acid-based polymeric arms emanating from a core comprising more than three arms,[23] and they are protein-like structures already recognized for their specific physical properties (hydrodynamic volumes, chain entanglement etc.)[24] or biological properties (antimicrobial, etc.).[25] To achieve the ROP, a dendritic core with "n" functional groups is often used, such as polyamidoamine to promote polymerization growth featuring primary/secondary amines as end groups.[26] Other initiators have also been used, including non-metalated porphyrins affording star-like polypeptides that will find use in drug-delivery for photodynamic therapy applications.[27] Nevertheless, porphyrins with amine functions (such as *5,10,15,20*-Tetrakis-(*4*-amininophenyl)-porphyrin or TAPP) are very hydrophobic, poorly soluble, and lack reactivity during the initiation step of the ring-opening polymerization. In this study, a small library of star-shaped polymers was accordingly prepared using a grafting-from approach with manganese(III) 5, 10, 15, 20-tetrakis-(4-aminophenyl)-porphyrin (Mn-TAPP) having 4-NH_2 terminal groups, from which 4 arms of polypeptides were synthesized trough ROP of γ-benzyl-*L*-glutamate *N*-carboxyanhydrides (BLG-NCAs, **Scheme 1**).

Star-like polypeptides with varying arm lengths were obtained by using a two-step synthetic methodology: in a first step, polymerization of BLG-NCA was performed in N,N-dimethyl formamide (DMF) at a concentration of 0.4 M and under inert conditions from Mn-TAPP. We monitored the monomer disappearance of the N-COO signal at 1850 cm^{-1} by Fourrier-transform infrared spectroscopy (FTIR) and we isolated the star-shaped polypeptides by precipitation drying under high vacuum and obtained in good yields (56%–94%). The polymers were characterized by size-exclusion chromatography (SEC)and ^{1}H-nuclear magnetic resonance (NMR) analyses (**Table 1** and **Figure 1**; Figures S1–S6, Supporting Information). This grafting-from approach was used to prepare a set of 3 star-shaped poly(γ-benzyl-*L*-glutamate) or PBLG varying arm lengths by targeting the following theoretical polymerization degrees (M/I or theoretical DP): 4-arm-PBLG DP = 10 (polym. **1**), 4-arm-PBLG DP = 25 (polym. **2**) and 4-arm-PBLG DP = 100 (polym **3**). These analyses evidenced polydispersity indexes $Đ_M$ (M_w/M_n) = 1.2–1.5, a good agreement of the polymer composition with the monomer feed ratio.

In a second step, water-soluble star-shaped polypeptides were obtained by deprotection of the PBLG arms, a post-polymerization reaction achieved in smooth acid medium using methane sulfonic acid (MSA), trifluoro acetic acid (TFA) and anisole. Upon this acidic deprotection and purification by dialysis, followed by freeze-drying, this reaction afforded 4-arm-PGA (PGA for poly(L-glutamic) acid): DP = 10 (polym **1′**, yield = 74%), 4-arm-PGA DP = 25 (polym **2′**, yield = 87%) and 4-arm-PGA DP = 100 (polym **3′**, yield = 94%). ^{1}H-NMR and SEC analyses confirmed that water-soluble star-like polypeptide with varying poly(glutamic acid) lengths were obtained (Figures 1 and 2): Polym. **1′** presented a number-average molecular weight (M_n) of 16 100 g mol^{-1}, polym. **2′** a molecular weight of M_n = 38 800 g mol^{-1} and polym. **3′** a molecular weight of M_n = 76 700 g mol^{-1}. All these M_n values were associated with $Đ_M$ lower than 1.4, an index value increasing with the length of the arms ($Đ_M$ = 1.20 for **1′** and up to 1.38 for **3′**), a feature already reported with star-like polymers.[28] The differences with $Đ_M$ values obtained before deprotection were attributed to the influence of the secondary structure in SEC performed in DMF (Table 1).[29] The star-shaped structures were further confirmed

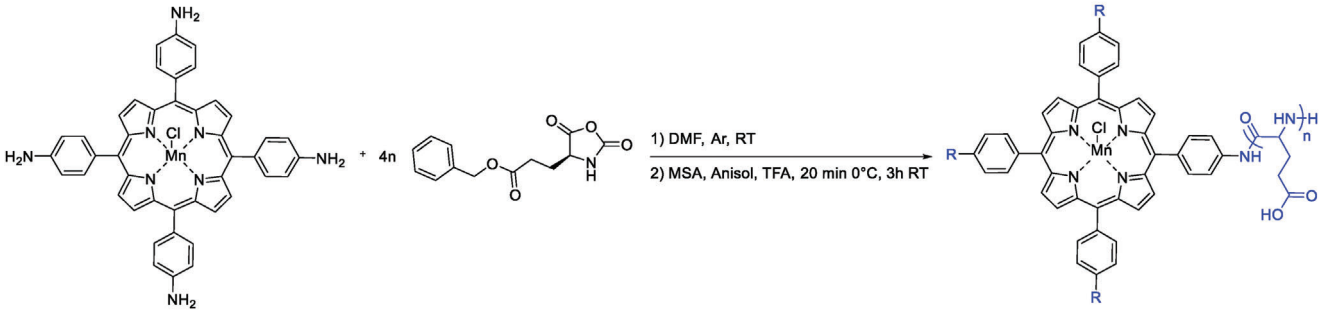

Scheme 1. Porphyrin-embedded, star-shaped multivalent polypeptides by using ring-opening polymerization from manganese porphyrin scaffolds: synthesis of PBLG by grafting-from Mn-TAPP.

Table 1. Star-like polymer characterization of polymers prepared by grafting-from Mn(III) porphyrins.

	M/I[a)]	MW_{theo} [kg mol^{-1}]	M_n [kg mol^{-1}]	M_w [kg mol^{-1}]	$Đ_M$	Yield
Polym **1**	10	9.8	36.4[b)]	42.8	1.18	56%
Polym **2**	25	22.7	30.2[b)]	48.5	1.60	88%
Polym **3**	100	88.4	85.1[b)]	130.5	1.53	84%
Polym **1**′	10	6.0	16.1[c)]	19.5	1.20	74%
Polym **2**′	25	13.7	38.8[c)]	52.7	1.36	87%
Polym **3**′	100	52.4	76.7[c)]	106.0	1.38	94%

[a)] Value determined from monomer/initiator ratio (M/I), where I it is correlated directly with the NH_2 groups; [b)] Polymers analyzed by SEC in DMF; [c)] Polymers analyzed by aqueous SEC.

by plotting the double logarithm of mean square radius (RMS radius) versus molar masses with polym. **1**–**3** and polym **1**′-**3**′(see Figures S7 and S8, Supporting Information).[30] We then investigated whether manganese remained in the porphyrin core and whether traces of demetallization could be observed during the deprotection process. Due to the paramagnetic nature of Mn(III), it was not possible to characterize the coordination by NMR. For this reason, we performed additional UV–vis spectroscopy analyses. They were carried out on the polymers **1**′-**3**′ and compared to Mn-TAPP spectrum measured in DMF as the porphyrin alone is not soluble in water. We did not observe the characteristic peaks of non-metalyzed porphyrin in the three solutions of polymers (see Figure S9, Supporting Information) and, in addition, the polymerization degree (DP) of the polymers was estimated before and after deprotection by using the molar attenuation coefficient (ϵ) of free Mn-TAPP at 484 nm and the Beer–Lambert law. Before acidic deprotection, UV–vis analyses indicated that star-like polypeptides were isolated, with a $DP_{per\ arm} = 9$ for Polym. **1**, $DP_{per\ arm} = 43$ for polym. **2** and $DP_{per\ arm} = 165$ for polym. **3** (see Table S1, Supporting Information).

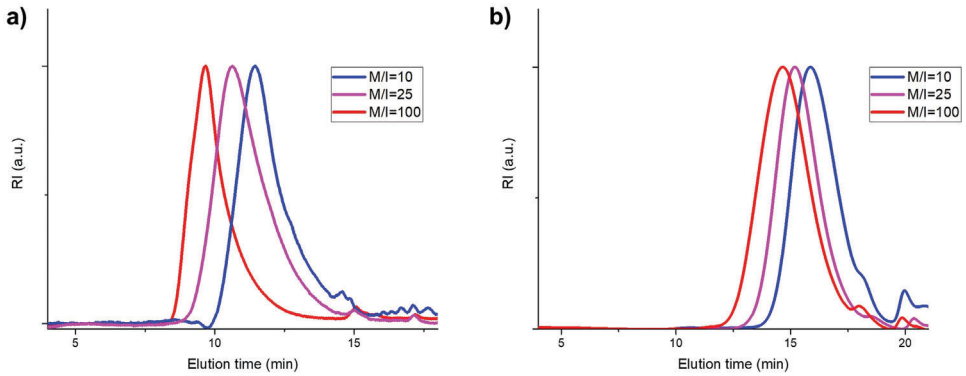

Figure 1. SEC characterization of star-like polypeptides prepared with Mn(III)-porphyrins: a) Refractive index trace profile of the star-like polymers at different M/I before deprotection from SEC in DMF; b) Refractive index trace profile of the star-like polymers at difference M/I upon deprotection from aqueous SEC.

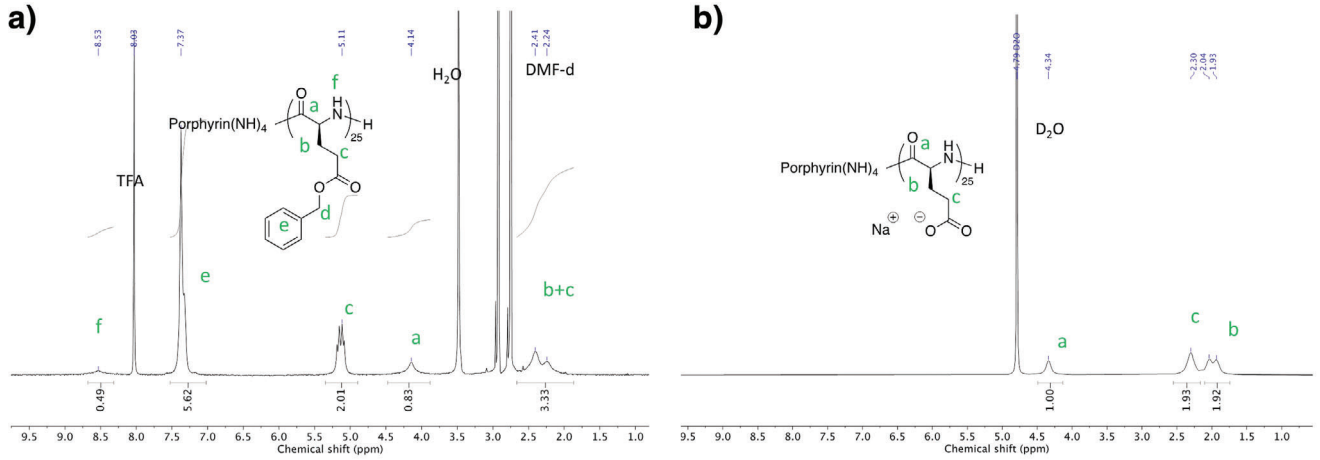

Figure 2. ^{1}H NMR analyses of star-like polypeptides prepared with Mn(III)-porphyrins: a) characteristic ^{1}H-NMR of star-like PBLG polymer at M/I = 25 before deprotection; and b) characteristic ^{1}H-NMR of star-like PGA polymer at M/I = 25 upon deprotection.

2.2. HRP-Like Catalytic Activity

Biocatalysis has a significant influence on a wide range of areas, including specialty chemicals,[31] cosmetics,[32] and drug preparation.[33] In principle, enzymatic catalysis provides access to very fast chemical conversions while preserving a chemical selectivity that few molecular systems are capable of reproducing.[34] However, the use of enzymes still suffers from significant limitations, including achieving modulation of the natural substrate selectivity. When enzymes are used, stability problems can also occur, becoming critical when implementing this type of catalysis in chemical engineering.[35] Peroxidase-type heme enzymes are not an exception, and there is a growing interest in finding new recombinant or artificial analogues of those oxidoreductases.[36] The most extensively studied peroxidase is HRP, that catalyzes the reaction between H_2O_2 and phenolic donors to yield phenoxyl radicals (and water). To study the enzymatic activity of HRP, it is also possible to use standard substrates such as 2,2′-azino-bis(3-ethylbenzothiazoline-6-sulphonique acid (ABTS))[37] or guaiacol, that upon oxidation yield colored compounds. [38] The products absorb at two specific wavelengths, i.e., 420 and 470 nm respectively. Indeed, ABTS and guaiacol are substrates of choice for quantifying the enzymatic activity, as their UV–vis monitoring is easy to set up and they do not auto-oxidize easily with H_2O_2, like other substrates readily found in the literature.[39] In this study, both substrates were used to evaluate and compare the H_2O_2-mediated catalytic oxidation activities of the star-shaped polypeptides with HRP. With the star-shaped polymers, the concentration of manganese porphyrin is a key factor to compare the catalytic activities and the concentrations used in the various biocatalysis assays are given below (**Table 2**).

As a control experiment, we first evaluated the catalytic efficiency of a fresh HRP solution (2.2 nM of heme residue) to convert either guaiacol (5 mM) or ABTS (1 mM) in presence of H_2O_2 (1 mM) in imidazole buffer solutions at a pH value of 6 (**Figure 3**). The reactions were monitored during 2 min using UV-spectroscopy (time 0 corresponded to the addition of H_2O_2). The rate was obtained by determining the slope at the origin and this value was used to calculate the initial rate Vi as well as the specific activity (amount of substrate transformed per heme units). Without enzyme, control kinetics indicated that under these experimental conditions, H_2O_2 was not able to achieve measurable oxidation of the two substrates (**Table 3**). HRP was found active in oxidizing both ABTS and guaiacol ($V_i = 11.10^{-5}$ M·min^{-1} and 9.10^{-5} M·min^{-1} respectively), in good agreement with the literature for this pH.[39] As already described, increasing the pH to a more basic value of 7 or 8 strongly decreased the oxidation activity on ABTS (Figure 3, $V_i = 1.10^{-5}$ M·min^{-1} instead of 11.10^{-5} M·min^{-1}) and significantly on guaiacol ($V_i = 5.10^{-5}$ M·min^{-1} instead of 9.10^{-5} M·min^{-1}).

We then investigated the catalytic activity of the polymers **1′-3′** in similar conditions. It is interesting to note that the use of H_2O_2 did not previously promote manganese porphyrin oxidation,[39] and that the native Mn-TAPP porphyrin used to build the star polymers is not water-soluble. We implemented the catalytic assays using polymer concentrations that were optimized to get the

Table 2. The different star polymers used in the catalytic tests: concentrations correspond to porphyrin concentrations measured by UV–vis.

	Mw (theo) in kg mol^{-1}	DP by UV measurements	[Heme (initial)] in μM	[Heme (final)] in μM
HRP	44	–	–	2.2×10^{-3}
Polym. 1′	6.0	9/arm	400	14.0
Polym. 2′	13.7	43/arm	50	1.7
Polym. 3′	52.4	165/arm	40	1.4

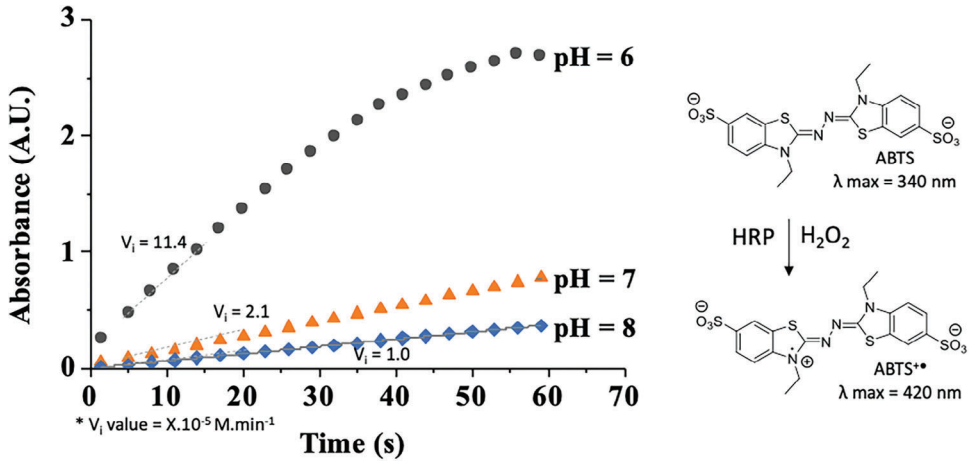

Figure 3. Rate of ABTS oxidation, catalyzed by HRP at different pH values in imidazole buffer.

speed in about 1–2 min: guaiacol (5 mM) or ABTS (1 mM) and H_2O_2 solution at 1 mM. In marked contrast to HRP, all the polymers were found to be almost inactive in oxidizing both ABTS and guaiacol at a pH value of 6 (**Table 4**), an expected behavior considering the literature.[39] However, and surprisingly, increasing the pH to 7 or 8 permitted to recover significant HRP-like activities (Table 4 and **Figure 4**). Indeed, increasing pH was found to strongly promote the oxidation with the star-like polypeptides and the best kinetics with both ABTS and guaiacol were measured at a pH value of 8: up to an activity of 11 $M{\cdot}M^{-1}{\cdot}min^{-1}$ using polymer **3′** and guaiacol or 8 $M{\cdot}M^{-1}{\cdot}min^{-1}$ using polymer **3′** and ABTS (Table 4). This better pH value of 8 for catalysis was presumably attributed to a synergy between the arms and the imidazole buffer with respect to coordination on the Mn(III) metallic center and the solubility of the polymer.

Comparing the length of the arms by comparing the kinetics monitored with **1′**, **2′** and **3′**, we observed another interesting effect: the longer arms optimized significantly the catalytic activity (for instance, guaiacol: 1.8 $M{\cdot}M^{-1}{\cdot}min^{-1}$ with **1′** to 11.6 $M{\cdot}M^{-1}{\cdot}min^{-1}$ with **3′**). A detailed analysis of the Soret bands shows a difference in coordination when the length of the arms changes (Figure S10, Supporting Information), confirming a confinement effect at the metalated porphyrin induced by the longer arms. Encouraged by these results, the robustness of the catalytic system was also assessed: a higher concentration of H_2O_2 (20 mM) was monitored with polymer **3′** with the two substrates(**Table 5** and **Figure 5**; Figure S11, Supporting Information) and compared to HRP.

Contrary to HRP, this higher amount of oxidant increased the activity of the polymer **3′** and allowed to obtain activities which were closer to the enzyme (for instance with ABTS, Table 5: 2300 $M{\cdot}M^{-1}{\cdot}min^{-1}$ with HRP as compared to 115 $M{\cdot}M^{-1}{\cdot}min^{-1}$ with polymer **3′**). In those optimized conditions, the efficacy difference factor was only 20 in favor of the HRP, a remarkable result in a context where usually stronger oxidants have to be used with artificial peroxidases based on Mn-TAPP (such as $KHSO_5$),[39] or more sensitive substrate (such as resorufin) using water soluble metalated porphyrins.[40]

2.3. Selectivity with Respect to H_2O_2

The Michaelis–Menten constant, denoted as K_M, is an important parameter in enzyme kinetics that depend on the affinity of an enzyme for its substrate. Typically, the K_M for HRP with H_2O_2 falls in the micromolar range,[41] and the K_M value varies depending on factors such as experimental conditions, assay setup, the reducing substrate and the specific type or source of HRP being used. Inspired by the catalytic performance obtained with polymer **3′**, kinetic studies carried out at different H_2O_2 concentrations were performed with guaiacol (5 mM) or ABTS (1 mM). A Lineweaver–Burk plot is depicted in **Figure 6** and it was used to calculate K_M constants for H_2O_2 of 45 mM when using guaiacol

Table 3. Kinetics of oxidations mediated by HRP with guaiacol and ABTS as substrates under three different pH conditions.

	Guaiacol			ABTS		
	Slope [Abs·min^{-1}]	*Vi* [M·min^{-1}][a)]	Specific activity [M·M^{-1}·min^{-1}][b)]	Slope [Abs·min^{-1}]	*Vi* [M·min^{-1}][c)]	Specific activity [M·M^{-1}·min^{-1}][d)]
Control (without enzyme)	–	–	–	–	–	–
pH 6	2.48	9.31×10^{-5}	4.23×10^{4}	4.09	11.37×10^{-5}	5.17×10^{4}
pH 7	1.96	7.35×10^{-5}	3.34×10^{4}	0.73	2.03×10^{-5}	0.92×10^{4}
pH 8	1.45	5.44×10^{-5}	2.47×10^{4}	0.37	1.03×10^{-5}	0.47×10^{4}

[a)] *Vi* value was obtained by dividing of the slope by $\epsilon = 26\,600$ M cm^{-1}; [b)] The specific activity was calculated by dividing the *Vi* value by the concentration of HRP (2.2 nM); [c)] *Vi* value was obtained by dividing of the slope by $\epsilon = 36\,000$ M cm^{-1}; [d)] The specific activity was calculated by dividing the *Vi* value by the concentration of HRP (2.2 nM).

Table 4. Kinetics of oxidations mediated by 4-arm-polypeptide **1′-3′** with guaiacol and ABTS as substrates under different pH conditions.

		Guaiacol			ABTS		
Polymer		Slope (Abs·min^{-1})	*Vi* (M·min^{-1})[a]	Specific activity (M·M^{-1}·min^{-1})	Slope (Abs·min^{-1})	*Vi* (M·min^{-1})[b]	Specific activity (M·M^{-1}·min^{-1})[d]
1′	pH 6	0.01	0.05×10^{-5}	3.57×10^{-2}[c]	–	–	–
	pH 7	0.26	0.99×10^{-5}	7.07×10^{-1}[c]	0.04	0.10×10^{-5}	7.14×10^{-2}[d]
	pH 8	0.68	2.55×10^{-5}	1.82[c]	0.16	0.45×10^{-5}	3.21×10^{-1}[d]
2′	pH 6	0.001	0.05×10^{-6}	2.94×10^{-2}[e]	–	–	–
	pH 7	0.07	0.27×10^{-5}	1.59[e]	0.01	0.02×10^{-5}	0.12[f]
	pH 8	0.29	1.11×10^{-5}	6.53[e]	0.28	0.76×10^{-5}	4.47[f]
3′	pH 6	0.003	0.12×10^{-6}	8.57×10^{-2} [g]	–	–	–
	pH 7	0.13	0.50×10^{-5}	3.57 [g]	0.13	0.35×10^{-5}	2.5 [h]
	pH 8	0.43	1.62×10^{-5}	11.6 [g]	0.40	1.12×10^{-5}	8 [h]

[a] *Vi* value was obtained by dividing the slope by $\epsilon = 26\,600$ M cm^{-1}; [b] *Vi* value was obtained by dividing the slope by $\epsilon = 36\,000$ M cm^{-1}; [c] The specific activity was calculated by dividing the *Vi* value by the concentration of polym. **1** (14 µM); [d] The specific activity was calculated by dividing the *Vi* value by the concentration of polym. **1** (14 µM); [e] The specific activity was calculated by dividing the *Vi* value with the concentration of polym. **2** (1.7 µM); [f] The specific activity was calculated by dividing the *Vi* value by the concentration of polym. **2** (1.7 µM); [g] The specific activity was calculated by dividing the *Vi* value by the concentration of polym. **3** (1.4 µM); [h] The specific activity was calculated by dividing the *Vi* value by the concentration of polym. **3** (1.4 µM).

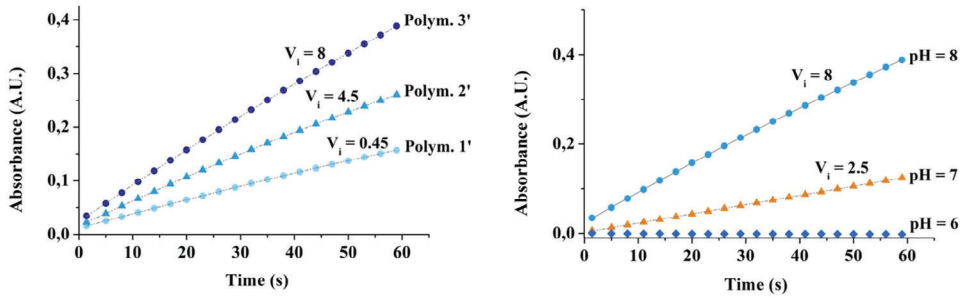

Figure 4. ABTS oxidation by star-shaped polypeptides **1′-3′**: A) comparison of kinetics obtained with the 3 polymers at pH 8 (note that the porphyrin concentration must be taken into account when calculating Vi; B) comparison of kinetics obtained with the most efficient polymer (**3′**) at different pH (here, the initial slope correlates the different Vi values obtained).

and of 16 mM when using ABTS as reducing substrate. Interestingly, control experiments in which the concentration of both guaiacol or ABTS substrates were changed showed no significant K_M (Figure S12, Supporting Information). Moreover, for comparison, the K_M constants of HRP was monitored in imidazole buffer at a pH value of 6 and found at 100 µM when using guaiacol and 11 µM when using ABTS (Figure S13, Supporting Information). In the end, the kcat/K_M ratio of polymer **3′** was calculated at 714 M^{-1} min^{-1} with guaiacol and 1155 M^{-1} min^{-1} with ABTS (see Table S3, Supporting Information). Although these biocatalytic efficiencies remains modest compared to the real enzyme, to the best of our knowledge, this is the first time that HRP-like catalytic effect is revealed with polypeptide polymers. This result evidences an exciting and original biomimetic lever to mimic HRP catalysis using simple polypeptide chemistry. With the polymers, the mM range affinity of H_2O_2 can have several origins, but the

Table 5. Kinetics of oxidations mediated by 4-arm-polypeptide **3′** or HRP under polymer optimized conditions (pH 8 and 20 mM H_2O_2) with guaiacol and ABTS as substrates.

		Guaiacol			ABTS		
		Slope (Abs·min^{-1})	*Vi* (M·min^{-1})[a]	Specific activity (M·M^{-1}·min^{-1})	Slope (Abs·min^{-1})	*Vi* (M·min^{-1})[b]	Specific activity (M·M^{-1}·min^{-1})[d]
	Control (without catalyst, pH 8)	–	–	–	–	–	–
HRP	20 mM H_2O_2 (pH 8)	1.37	5.14×10^{-5}	2.3×10^{4}	0.18	0.5×10^{-5}	0.2×10^{4}
Polymer **3′**	20 mM H_2O_2 (pH 8)	3.84	14.44×10^{-5}	0.1×10^{4}	5.81	1.61×10^{-4}	115

[a] *Vi* value was obtained by dividing of the slope by $\epsilon = 26\,600$ M cm^{-1}; [b] The specific activity was calculated by dividing of the *Vi* value with the concentration of polymer **3** (1.4 µM); [c] *Vi* value was obtained by dividing of the slope by $\epsilon = 36\,000$ M cm^{-1}; [d] The specific activity was calculated by dividing of the *Vi* value with the concentration of polymer **3** (1.4 µM) or with the concentration of HRP (2.2 nM).

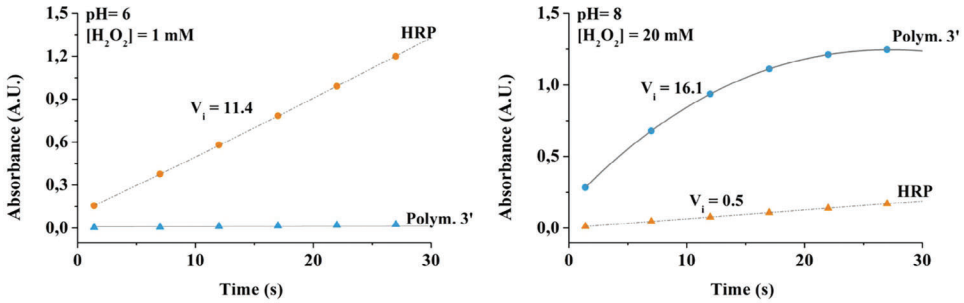

Figure 5. Guaiacol oxidation by star-shaped polypeptides **3′** versus HRP: A) comparison of kinetics obtained in the best conditions for HRP; B) comparison of kinetics obtained in the best conditions for polymer (note that the porphyrin concentration is much higher in the case of **3′**: 1.4 µM (compared to 2.2 nM for HRP).

K_M value obtained with **3′** was interestingly linked to the length of the polymer arms and somehow to a spatial constrain brought by such star-shaped structure, a behavior already known with dendritic structures.[28]

2.4. Star-Like Polypeptide as Fully Peptidic But More Robust Analogues of HRP

As depicted in Figure 5, increasing the H_2O_2 by a concentration factor of 20 at a pH value of 6 did not improve the kinetic of oxidation reaction for HRP and even decreased it strongly in the case of ABTS. As already discussed in Section 2.2, this result shows that the polymer system has greater robustness with respect to the substrate concentration, a robustness that can be explained by the lower K_M values (Section 2.3) but that can also be explained by the synthetic star-shaped topology, which unfolds and degrades less easily than the natural enzyme. To better understand and compare the limitations of the HRP system, we also evaluated the catalytic efficiency of HRP solution after a denaturing treatment at 80 °C. After this treatment, kinetics were monitored to convert either guaiacol (5 mM) or ABTS (1 mM) in presence of H_2O_2 (1 mM) in imidazole buffer solutions at a pH value of 6 (**Table 6**). For the two substrates, the denaturing treatment completely eliminated the catalytic activity. This was found in marked contrast to the star-shaped catalysts **1′**-**3′** that did not show any loss of activity after similar heat treatment (Table 6; Figure S14, Supporting Information). For instance, with **3′**, the oxidation activity on ABTS was found at 9.2 M M^{-1} min^{-1} after the denaturing treatment a value that was close to 8 M M^{-1} min^{-1} calculated on kinetics performed without the heat treatment. The higher residual activity was attributed to a solubilization phenomenon of the polymers optimizing the catalysis.

To take this a stepfurther, degradation studies using denaturing agents or proteases were finally carried out on the polymer **3′**. First, the use of a urea pre-treatment did not modify the catalytic activity (whereas this non-thermal treatment modified the HRP activity, data not showed). This means that the star-shaped polymer catalyst was less sensitive to denaturing conditions than the natural protein. On the other hand, proteinase K, which is a protease able to hydrolyze the amide bond when encountering aliphatic or aromatic amino acid residues in position P1, showed that the copolymer is stable to proteolysis, as evidenced by the SDS page gel shown in **Figure 7**.

Overall, these data show that the polymer system can be a more robust system than HRP for carrying out H_2O_2-mediated oxidation of ABTS and guaiacol.

3. Conclusion

We have successfully prepared star-shaped polymeric analogues of HRP capable of undergoing oxidation reactions with H_2O_2. This biomimetic reactivity, although less efficient than that of the enzyme, is exceptional for a synthetic system involving Mn(III) porphyrins. This holds great promise when using high concentrations of H_2O_2 or when considering the more robust nature of the polymer with respect to temperature changes, denaturing agents or proteolysis. Based on the same structural elements (polypeptide + metalated porphyrins), we believe that our simplified analogues of HRP pave the way for a much better

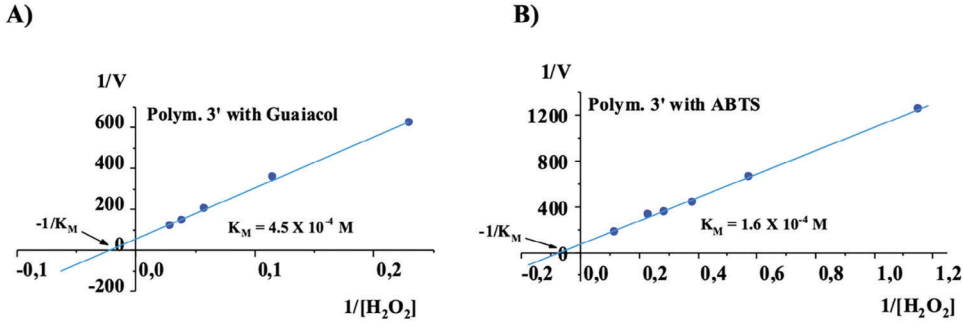

Figure 6. Lineweaver–Burk plot of the H_2O_2-mediated oxidation of guaiacol (A) and ABTS (B) using polymer **3′**.

Table 6. Kinetics of oxidations mediated by 4-arm-polypeptide **3′** with guaiacol and ABTS as substrates after heating the catalyst at 80 °C and 30 min before use (pH 6 for HRP or 8 for **3′** and 1 mM H_2O_2).

		Guaiacol			ABTS		
		Slope (Abs·min^{-1})	*Vi* (M·min^{-1})[a)]	Specific activity (M·M^{-1}·min^{-1})	Slope (Abs·min^{-1})	*Vi* (M·min^{-1})[b)]	Specific activity (M·M^{-1}·min^{-1})[d)]
	Control (without enzyme)	–	–	–	–	–	–
HRP	**pH 6**	2.48	9.3×10^{-5}	4.23×10^{4}	4.09	11.4×10^{-5}	5.17×10^{4}
	Upon heating (pH 6)	–	–	–	–	–	–
Polymer **3′**	**pH 8**	0.43	1.6×10^{-5}	11.6	0.40	1.1×10^{-5}	8
	Upon heating (pH 8)	0.49	1.8×10^{-5}	13.2	0.46	1.3×10^{-5}	9.2

[a)] *Vi* value was obtained by dividing of the slope by $\epsilon = 26\,600$ M cm^{-1}; [b)] The specific activity was calculated by dividing of the *Vi* value with the concentration of polymer **3′** (1.4 µM); [c)] *Vi* value was obtained by dividing of the slope by $\epsilon = 36\,000$ M cm^{-1}; [d)] The specific activity was calculated by dividing of the *Vi* value with the concentration of polymer **3′** (1.4 µM) or with the concentration of HRP (2.2 nM).

storage principle, while retaining the recyclability of a structure composed entirely of amino acids.

4. Experimental Section

Materials and Methods: Mn-TAPP, BLG-NCA, H_2O_2 30%, imidazole, ABTS, guaiacol and HRP were purchased from Porphychem, PMC Isochem, Sigma-Aldrich. Proteinase K was acquired from ThermoScientific. Bio-Rad Protein Assay Dye Reagent Concentrated from Bio-Rad, USA. All chemicals were used without any further purification. The infrared spectra were recorded using an FTIR spectrometer (Vertex 70, Bruker), and the samples were measured with an ATR (GladiATR, Pike Technologies) from Fisher technologies performing 32 scans at the LCPO (Bordeaux, France). The raw data were obtained with Opus7.5 software and processed using Originlab 2016 software. The NMR spectra were recorded using a Bruker Avance III 400 spectrometer (LCPO, Bordeaux, France). The spectra were obtained at 22 °C and data was analyzed using Mestrenova 14.1.2 software. The chemical shifts of the signals are given in ppm. The spectra obtained were calibrated using the residual solvent signals ($CHCl_3$ 7.26 ppm, H_2O 4.79 ppm, DMSO-d_6 2.50 ppm). The signals were categorized as follows: singlet (s), doublet (d), triplet (t), quartet (q), multiplet (m) and broad (br). Polymer molar masses were determined by size exclusion chromatography (SEC) using: (a) dimethylformamide (DMF + lithium bromide LiBr 1 g L^{-1}) as the eluent (LCPO, Bordeaux, France). Measurements in DMF were performed on an Ultimate 3000 system from Thermoscientific equipped with diode array detector DAD. The system also included a multiangle light scattering detector MALS and differential refractive index detector dRI from Wyatt technology. Polymers were separated on two Shodex Asahipack gel columns GF310 and GF510 (300 Å–7.5 mm) (exclusion limits from 500 Da to 300 000 Da) at a flow rate of 0.5 mL min^{-1}. Column temperature was held at 50 °C. The chromatograms were recorded with Chromeleon 7.2 software and Astra 7.1.0 software and analyzed using Originlab 2016 software. The *dn/dc* were determined experimentally. (b) Hexafluoro-2-propanol (HFIP + 0.05% KTFA) as the eluent (LCPO, Bordeaux, France). Measurements in HFIP were performed on an Ultimate 3000 system from Thermoscientific equipped with diode array detector DAD. The system also included a multi-angle light scattering detector MALS and differential refractive index detector dRI from Wyatt technology. Polymers were separated on PL HFIP gel column (300 Å–7.5 mm) (exclusion limit from 100 to 150 000 Da) at a flow rate of 0.8 mL min−1. Column temperature was held at 40 °C. The chromatograms were recorded with Chromeleon 7.2 software and Astra 7.1.0 software and analyzed using Originlab 2016 software. The molar mass was calculated using either a calibration curve or the *dn/dc* value. The calibration curve was performed with polystyrene standards with molar masses in the range 0.9–364 kg mol−1. The dn/dc were determined experimentally.

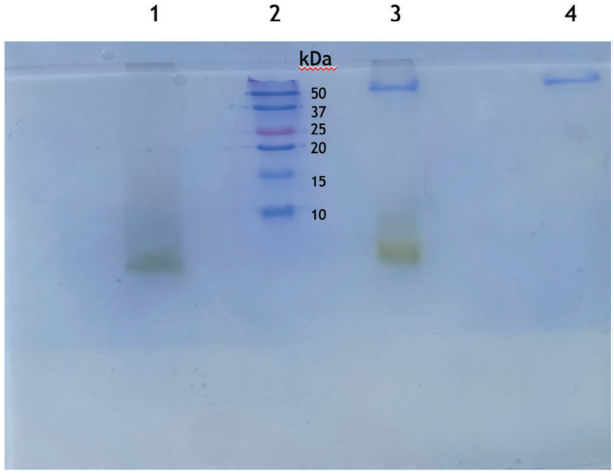

Figure 7. SDS-PAGE, 18% acrylamide. *Lane 1*, polymer **3′**; *Lane 2*, molecular weight marker; *Lane 3*, polymer **3′** after proteinase K treatment; *Lane 4*, proteinase K alone as control.

Synthesis Procedures: *Synthesis of Mn-TAPP-PBLG* ***1***. In a flame-dried Schlenk under pure argon, Manganese(III) 5, 10, 15, 20-Tetrakis-(4-aminophenyl)-porphyrin chloride (36 mg, 4.7×10^{-5} mol) was added and dried under high vacuum for 1 h. Then, 5 mL of BLG-NCA monomer 0.4 M in anhydrous DMF (0.5 g, 1.9×10^{-3} mol) was added with an argon purged syringe. The solution was stirred at room temperature under argon until the disappearance of the peak around 1850 cm^{-1}, observed by FTIR. The polymer was then recovered by precipitation twice in 40 mL of diethyl ether, centrifuged and dried under high vacuum. Yield: 56%. The representative ^{1}H NMR of the PBLG backbone signals were observed in DMF-d7 (400 MHz, δ, ppm): 8.53 (br s, 1H, NH), 7.60–7.11 (m, 5H, benzyl), 5.37–4.97 (m, 2H, benzyl), 4.14 (br s, 1H, CH), 2.58–2.12 (m, 4H, 2 CH_2).

Synthesis of Mn-TAPP-PGA ***1′***. Mn-TAPP-PBLG **1** (201 mg; 9.1×10^{-4} mol of BLG units) were dissolved in 2 mL of TFA. The solution was stirred at 0 °C for 20 min, and 0.4 mL of anisole and 2 mL of MSA were added and the reaction mixture was stirred for 20 min at 0 °C, followed by stirring during 40 min at room temperature. Then, the polymer was precipitated twice in 40 mL of diethyl ether, centrifuged and dried under high vacuum. The polymer was suspended in water, neutralized at pH 7 with a saturated solution of $NaHCO_3$ dialyzed against milliQ water (MWCO 1,0 kDa) and freeze-dried yielding green powder (74% yield). The representative ^{1}H NMR of the poly(L-glutamic acid) backbone signals were observed in D_20 (400 MHz, δ, ppm): 4.34 (br, 1H, CH), 2.30 (br, 2H, CH_2), 1.93 (br, 2H, CH_2). The NH group was not observed under the experimental conditions.

Synthesis of Mn-TAPP-PBLG **2.** In a flame-dried Schlenk under pure argon, Manganese(III) 5, 10, 15, 20-Tetrakis-(4-aminophenyl)-porphyrin chloride (7.2 mg, 9.4×10^{-6} mol) was added and dried under high vacuum for 1 h. Then, 2.5 mL of BLG-NCA 0.4 M in anhydrous DMF (0.25 g, 9.5×10^{-4} mol) was added with an argon purged syringe. The solution was stirred at room temperature under argon until the disappearance of the peak around 1850 cm^{-1} by FTIR. The polymer was then recovered by precipitation twice in 40 mL of diethyl ether, centrifuged and dried under high vacuum. Yield: 88%. The representative ^{1}H NMR of the PBLG backbone signals were observed in DMF-d7 (400 MHz, δ, ppm): 7.60–7.11 (m, 5H, benzyl), 5.37–4.97 (m, 2H, benzyl), 4.15 (br s, 1H, CH), 2.58–2.12 (m, 4H, 2 CH_2). The NH group was not observed under the experimental conditions.

Synthesis of Mn-TAPP-PGA **2′**. Mn-TAPP-PBLG **2** (100 mg; 4.5×10^{-4} mol of BLG units) was dissolved in 1 mL of TFA. The solution was stirred at 0 °C for 20 min, and 0.2 mL of anisole and 1 mL of MSA were added and the reaction mixture was stirred for 20 min at 0 °C followed by stirring for 40 min at room temperature. Then, the polymer was precipitated twice in 40 mL of diethyl ether, centrifuged and dried under high vacuum. The polymer was suspended in water, neutralized at pH 7 with a saturated solution of $NaHCO_3$ dialyzed against milliQ water (MWCO 1,0 kDa) and freeze-dried yielding green powder (87% yield). The representative ^{1}H NMR of the poly(L-glutamic acid) backbone signals were observed in D_20 (400 MHz, δ, ppm): 4.34 (br, 1H, CH), 2.29 (br, 2H, CH_2), 1.90 (br, 2H, CH_2). The NH group was not observed under the experimental conditions.

Synthesis of *Mn-TAPP-PBLG* **3**. In a flame-dried Schlenk under pure argon, Manganese(III) 5, 10, 15, 20-Tetrakis-(4-aminophenyl)-porphyrin chloride (3.6 mg, 4.7×10^{-6} mol) was added and dried under high vacuum for 1 h. Then, 5 mL of BLG-NCA monomer 0.4 M in anhydrous DMF (BLG-NCA, 0.5 g, 1.9×10^{-3} mol) was added with an argon purged syringe. The solution was stirred at room temperature under argon until the disappearance of the peak around 1850 cm^{-1} by FTIR. The polymer was then recovered by precipitation twice in 40 mL of diethyl ether, centrifuged and dried under high vacuum. Yield: 84%. The representative ^{1}H NMR of the PBLG backbone signals were observed in DMF-d7 (400 MHz, δ, ppm): 8.50 (br s, 1H, NH), 7.60–7.11 (m, 5H, benzyl), 5.37–4.97 (m, 2H, benzyl), 4.11 (br s, 1H, CH), 2.58–2.12 (m, 4H, 2 CH_2)

Synthesis of Mn-TAPP-PGA **3′**. Mn-TAPP-PBLG **3** (100 mg; 4.5×10^{-4} mol of BLG units) was dissolved in 1 mL of TFA. The solution was stirred at 0 °C for 20 min, and 0.2 mL of anisole and 1 mL of MSA were added and the reaction mixture was stirred for 20 min at 0 °C followed by stirring for 40 min at room temperature. Then, the polymer was precipitated twice in 40 mL of diethyl ether, centrifuged and dried under high vacuum. The polymer was suspended in water, neutralized at pH 7 with a saturated solution of $NaHCO_3$ dialyzed against milliQ water (MWCO 1,0 kDa) and freeze-dried yielding green powder (94% yield). The representative ^{1}H NMR of the poly(L-glutamic acid) backbone signals were observed in D_20 (400 MHz, δ, ppm): 4.35 (br, 1H, CH), 2.31 (br, 2H, CH_2), 2.02 (br, 2H, CH_2). The NH group was not observed under the experimental conditions.

Enzymatic/Catalytic Activities: *HRP Solution*: HRP suspension (100 µL) were diluted in 900 µL of phosphates buffer pH 7.0. The concentration of this solution was estimated from a calibration curve using the Bradford methodology, having a final concentration of 32 µg mL^{-1}.

HRP Kinetics: Two methodologies were employed to follow the kinetics of the HRP: A) Using guaiacol, in a Eppendorf tube 957 µL of imidazole buffer (0.1 M), 30 µL of guaiacol (mother solution: 160 mM) and 3 µL of HRP (mother solution: 7.3×10^{-7} M) were placed and this solution was extracted as baseline. Then, 10 µL of H_2O_2 (mother solution: 0.1 M) were added and the evolution of the absorbance value was monitored at 470 nm. B) Using ABTS, in an Eppendorf tube 965 µL of imidazole buffer (0.1 M), 20 µL of ABTS (mother solution: 50 mM) and 3 µL of HRP (7.3×10^{-7} M) were placed and this solution was extracted as baseline. Then, 10 µL of H_2O_2 (mother solution: 0.1 M) were added and the evolution of the absorbance value was monitored at 420 nm. The kinetics were recorded in a 8543 UV–vis Spectrophotometer from Agilent technologies and the data was processed with the UV–vis ChemStation Software.

Polymers kinetics: Two methodologies were employed to follow the kinetics of the star-like polypeptides: A) in an Eppendorf tube 920 µL of imidazole buffer (0.1 M), 30 µL of guaiacol (mother solution: 160 mM) and 35 µL of polymer solution (varying µM, depending on the star-like polypeptide, see Table 2, final concentration column) were placed and this solution was extracted as baseline. Then, 10 µL of H_2O_2 (mother solution: 0.1 M) were added and the evolution of the absorbance value was monitored at 470 nm. B) in a Eppendorf tube 940 µL of imidazole buffer (0.1 M), 20 µL of ABTS (50 mM) and 35 µL of polymer solution (varying µM, depending on the star-like polypeptide, see Table 2, final concentration column) were placed and this solution was extracted as baseline. Then, 5 µL of H_2O_2 (mother solution: 0.1 M) were added and the evolution of the absorbance value was monitored at 420 nm.

Effect of the Temperature: The kinetics were performed upon incubation of the enzyme or polymer with the buffer at 80 °C for 30 min. Then, guaiacol or ABTS were added and the base line was extracted, followed by the addition of H_2O_2. The initial rate was recorded in the spectrophotometer.

Effect of High Concentration of H_2O_2 with ABTS and guaiacol: The final H_2O_2 concentration was changed to 0.02 M (2.3 µL of an 8.8 M stock solution). The difference in volume was then added by adding more of the corresponding imidazole buffer.

Km Determination: For Km and catalytic efficiency (kcat Km^{-1}) determination, the initial reaction rate was measured at different H_2O_2 concentrations, from 0.5 to 40 mM for polymer **3′** and 1 to 200 µM for HRP, while maintaining the catalyst and organic substrate concentration in constant values (guaiacol 5 mM or ABTS 1 mM). The resulting data was graphed according to the inverse reciprocal equation from Lineweaver–Burk, and a straight line was adjusted in order to calculate the value of Km from the intercept (-1 Km^{-1}) with the *x* axis and the value of kcat Km^{-1} from the inverse of the slope (Km $kcat^{-1}$), considering the amount of each catalyst in the reaction.

Proteolysis and Gel Electrophoresis: Proteolysis resistance of the catalyst was tested for polymer 3′. Proteinase K was incubated with polymer 3′ under the following conditions: 14 µg mL^{-1} of polymer 3′ in 10 mM Tris buffer, pH 7.5 containing 1 mM $CaCl_2$ and 150 µg mL^{-1} of proteinase K, for 1 h at 40 °C. According to the vendor recommendations, typical working concentration for proteinase K is 50–100 µg ml^{-1}. The mixture reaction, along with controls, were analyzed in a 18% acrylamide SDS-PAGE.

Supporting Information

Supporting Information is available from the Wiley Online Library or from the author.

Acknowledgements

The authors acknowledge Genevieve Pratviel and Pierre Verhaeghe for their fruitful support and discussions. This work was supported by the ECOS Nord exchange program (grant M19P05 and 299050) and by the IEA P2NanoBio. P.S.A. received support from CONACYT (scholarship holder No. 548662).

Conflict of Interest

The authors declare no conflict of interest.

Data Availability Statement

The data that support the findings of this study are available from the corresponding author upon reasonable request.

Keywords

biocatalysis, N-carboxyanhydrides, protein-like polymers, ring-opening polymerization, star-like polypeptide

Received: April 1, 2024
Revised: June 19, 2024
Published online: August 9, 2024

[1] C. B. Castro, M. P. Ferreira, C. G. C. Marques Netto, *Curr. Res. Chem. Biol.* **2021**, *1*, 100004.
[2] S. K. Chapman, S. Daff, A. W. Munro, *Struct. Bond.* **1997**, *88*, 39.
[3] J. W. Adamson, C. A. Finch, *Rev. Physiol.* **1975**, *37*, 351.
[4] H. B. Gray, J. R. Winkler, *Annu. Rev. Biochem.* **1996**, *65*, 537.
[5] T. L. Poulos, *Chem. Rev.* **2014**, *114*, 3919.
[6] G. R. Lopes, D. C. G. A. Pinto, M. S. Silva, *RSC Adv.* **2014**, *4*, 37265.
[7] L. A. Sternberger, P. H. Hardy, J. J. Cuculis, H. G. Meyer, *J. Histochem. Cytochem.* **1970**, *18*, 333.
[8] S. Lv, D. Li, H. Ju, Y. Ma, C. Qiu, G. Zhang, *J. Appl. Polym. Sci.* **2013**, *128*, 529.
[9] B. Tang, Y. Wang, H. Liang, Z. Chen, X. He, H. Shen, *Spectrochim. Acta, Part A* **2006**, *63*, 609.
[10] H. Krishna, P. Nagaraja, A. Shivakumar, K. Avinash, V. Lingaiah, *J. Chin. Chem. Soc.* **2013**, *60*, 452.
[11] R. J. Dai, H. Huang, J. Chen, Y. L. Deng, S. Y. Xiao, *Chin. J. Chem.* **2007**, *25*, 1690.
[12] a) L. Casella, M. Gullotti, L. De Gioia, R. Bartesaghi, F. Chillemi, *J. Chem. Soc., Dalton Trans.* **1993**, *14*, 2233; b) K. Tomizaki, H. Nishino, T. Kato, A. Miike, N. Nishino, *Chem. Lett.* **2000**, *6*, 648; c) N. Umezawa, N. Matsumoto, S. Iwama, N. Kato, T. Higushi, *Bioorg. Med. Chem.* **2010**, *18*, 6340.
[13] D. Jiang, D. Ni, Z. T. Rosenkrans, P. Huang, X. Yan, W. Cai, *Chem. Soc. Rev.* **2019**, *48*, 3683.
[14] M. Chino, L. Leone, G. Zambrano, F. Pirro, D. D'Alonzo, V. Firpo, D. Aref, L. Lista, O. Maglio, F. Nastri, A. Lombardi, *Biopolymers* **2018**, *109*, e23107.
[15] A. Lombardi, F. Nastri, V. Pavone, *Chem. Rev.* **2001**, *101*, 3165.
[16] a) Y. Lu, N. Yeung, N. Sieracki, N. M. Marshall, *Nature* **2009**, *460*, 855; b) V. Nanda, R. L. Koder, *Nat. Chem.* **2010**, *2*, 15; c) Y. W. Lin, *Chem. Eng. J.* **2017**, *336*, 1; d) P. Dydio, H. M. Key, A. Nazarenko, J. Y.-E. Rha, V. Seyedkazemi, D. S. Clark, J. F. Hartwig, *Science* **2016**, *354*, 102.
[17] A. Rasines Mazo, S. Allison-Logan, F. Karimi, N. Jun-An Chan, W. Qiu, W. Duan, N. M. O'Brien-Simpson, G. G. Qiao, *Chem. Soc. Rev.* **2020**, *49*, 4737.
[18] W. Wu, W. Wang, J. Li, *Prog. Polym. Sci.* **2015**, *46*, 55.
[19] C. Bonduelle, *Polym. Chem.* **2018**, *9*, 1517.
[20] C. Bonduelle, F. Makni, L. Severac, E. Piedra-Arroni, C. L. Serpentini, S. Lecommandoux, G. Pratviel, *RCS Adv.* **2016**, *6*, 84694.
[21] J. Aujard-Catot, M. Nguyen, C. Bijani, G. Pratviel, C. Bonduelle, *Polym. Chem.* **2019**, *9*, 4100.
[22] G. Manai, H. Houimel, M. Rigoulet, A. Gillet, P. F. Fazzini, A. Ibarra, S. Balor, P. Roblin, J. Esvan, Y. Coppel, B. Chaudret, C. Bonduelle, S. Tricard, *Nat. Commun.* **2020**, *11*, 2051.
[23] J. M. Ren, T. G. McKenzie, Q. Fu, E. H. H. Wong, J. Xu, Z. An, S. Shanmugam, T. P. Davis, C. Boyer, G. G. Qiao, *Chem. Rev.* **2016**, *116*, 6743;
[24] K. Aoi, T. Hatanaka, K. Tsutsumiuchi, M. Okada, T. Imae, *Macromol. Rapid Commun.* **1999**, *20*, 378.
[25] S. J. Lam, N. M. O'Brien-Simpson, N. Pantarat, A. Sulistio, E. H. H. Wong, E. C. Reynolds, G. G. Qiao, *Nat. Microbiol.* **2016**, *1*, 1.
[26] P. Salas-Ambrosio, A. Tronnet, M. Badreldin, L. Reyes, M. Since, S. Bourgeade-Delmas, B. Dupuy, P. Verhaeghe, C. Bonduelle, *Polym. Chem.* **2022**, *13*, 600.
[27] a) C. S. Lee, W. Park, S. J. Park, K. Na, *Biomaterials* **2013**, *34*, 9227; b) X. H. Dai, W. H. Yang, C. Wu, D. D. Chang, Y. R. Dai, J. M. Pan, Y. S. Yan, *J. Photopolym. Sci. Technol.* **2016**, *29*, 823; c) Y. Zheng, Z. Li, H. Chen, Y. Gao, *Eur. J. Pharm. Sci.* **2020**, *144*, 105213.
[28] S. Hietala, S. Strandman, P. Järvi, M. Torkkeli, K. Jankiva, S. Hvilsted, H. Tenhu, *Macromolecules* **2009**, *42*, 1726.
[29] D. Huesmann, A. Birke, K. Klinker, S. Türk, H. J. Räder, M. Barz, *Macromolecules* **2014**, *47*, 928.
[30] S. Podzimek, T. Vlcek, C. Johann, *J. Appl. Polym. Sci.* **2001**, *81*, 1588.
[31] S. Wu, R. Snajdrova, J. C. Moore, K. Baldenius, U. T. Bornscheuer, *Angew. Chem., Int. Ed.* **2021**, *60*, 88.
[32] P. L. Gupta, M. Rajput, T. Oza, U. Trivedi, G. Sanghvi, *Nat. Prod. Bioprospect.* **2019**, *9*, 267.
[33] J. P. Adams, M. J. B. Brown, A. Diaz-Rodriguez, R. C. Lloyd, G. D. Roiban, *Adv. Synth. Catal.* **2019**, *361*, 2421.
[34] P. R. Ortiz de Montellano, *Chem. Rev.* **2010**, *110*, 932.
[35] M. T. Reetz, *Chem. Rec.* **2016**, *16*, 2449.
[36] K. Juarez-Moreno, M. Ayala, R. Vazquez-Duhalt, *Appl. Biochem. Biotech.* **2015**, *177*, 1364.
[37] E. N. Kadnikova, N. M. Kostić, *J. Mol. Catal. B Enzym.* **2002**, *18*, 39.
[38] H. Tonami, H. Uyama, R. Nagahata, S. Kobayashi, *Chem. Lett.* **2004**, *33*, 796.
[39] R. Song, A. Robert, J. Bernadou, B. Meunier, *Inorganica Chemica Acta* **1998**, *272*, 228.
[40] I. N. Westensee, L. J. Paffen, S. Pendlmayr, P. De Dios Andres, M. A. Ramos Docampo, B. Städler, *Adv. Healthcare Mater.* **2024**, *13*, 2303699.
[41] D. Morales-Urrea, A. Lopez-Cordoba, E. M. Contreras, *Sci. Rep.* **2023**, *13*, 13363.